Available online at www.sciencedirect.com
SCIENCE DIRECT
Biochemical Pharmacology 68 (2004) 1845–1855
Biochemical Pharmacology
www.elsevier.com/locate/biochempharm

Cadmium induces apoptotic cell death in WI 38 cells via caspase-dependent Bid cleavage and calpain-mediated mitochondrial Bax cleavage by Bcl-2-independent pathway

Seon-Hee Oh[a,*], Byung-Hoon Lee[b], Sung-Chul Lim[a]

[a]*Research Center for Resistant Cells, College of Medicine, Chosun University, Seosuk-dong, Dong-gu, Gwangju 501-759, South Korea*
[b]*Laboratory of Hygienic Pharmacy and Molecular Toxicology, College of Pharmacy, Wonkwang University, Iksan, Jeonbuk 570-749, South Korea*

Received 27 March 2004; accepted 7 June 2004

Abstract

Previous reports have demonstrated that cadmium (Cd) may induce cell death via apoptosis, but the mechanism responsible for cellular death is not clear. In this study, we investigated the signaling pathways implicated in Cd-induced apoptosis in lung epithelial fibroblast (WI 38) cells. Apoptotic features were observed using terminal deoxynucleotidyl transferase-mediated dUTP nick-end labeling assay, propidium iodide staining and DNA laddering. A treatment of cadmium caused the caspase-8-dependent Bid cleavage, the release of cytochrome *c* (Cyt *c*), activation of caspase-9 and -3, and PARP cleavage. A caspase-8 specific inhibitor prevented the Bid cleavage, caspase-3 activation and cell death. Alternatively, we observed that full-length Bax was cleaved into 18-kDa fragment (p18/Bax); this was initiated after 12 h and by 36 h the full-length Bax protein was totally cleaved to the p18/Bax, which caused a drastic release of Cyt *c* from mitochondria. The p18/Bax was detected exclusively in the mitochondrial fraction, and it originated from mitochondrial full-length Bax, but not from the cytosol full-length Bax. Cd also induced the activation of the mitochondrial 30-kDa small subunit of calpain that was preceded by Bax cleavage. Cd induced the upregulation of Bcl-2 and the degradation of p53 protein. *N*-acetyl cysteine effectively inhibited the Cd-induced $\Delta\Psi_m$ reduction, indicating ROS acts upstream of mitochondrial membrane depolarization. Taken together, our results suggest that Cd-induced apoptosis was thought to be mediated at least two pathways; caspase-dependent Bid cleavage, and the other is calpain-mediated mitochondrial Bax cleavage. Moreover, we found that the function of Bid and Bax was not dependent of Bcl-2, and that ROS can also contribute in the Cd-induced cell death.

Keywords: Cadmium; Apoptosis; Caspase; Bax cleavage; Calpain; Lung epithelial fibroblast (WI 38) cell

1. Introduction

Cadmium (Cd) is a widespread environmental and industrial pollutant that has been classified as a type I carcinogen by the International Agency for Cancer Research [1]. The primary routes of cadmium exposure in humans are via inhalation from such sources as cigarette smoking, and the ingestion of Cd containing food [2,3]. Only about 5% of a given dosage of Cd is absorbed from the gastrointestinal tract, while lung absorption is as much as 90% of a dose inhaled into the lungs. Despite being one of the major routes for Cd absorption, the toxic mechanism of Cd on lung tissue is still poorly understood.

Apoptosis does not only play an essential role in development and tissue homeostasis but it is also involved in a wide range of pathological conditions [4,5]. Typically, two different apoptosis signaling pathways are activated depending on the death stimuli, that is, death receptor-mediated signal and death receptor-independent signal via the mitochondria. The ligation of the

Abbreviations: Cd, cadmium acetate; Cyt *c*, cytochrome *c*; ROS, reactive oxygen species; MTT, 3-(4,5-dimethyl- thiazole-2-yl)-2,5-diphenyltetrazolium bromide; PBS, phosphate buffered saline; PI, propidium iodide; zVAD-fmk, *N*-benzyloxycarbonyl-Val-Ala-Asp-fluoromethylketone; zIETD-fmk, *N*-benzyloxycarbonyl-IIe-Glu-Thr-Asp-fluoromethylketone; MPT, mitochondrial permeability transition; PARP, poly(ADP-ribose)polymerase; $\Delta\Psi_m$, mitochondrial transmembrane potential; DCFH-DA, dichlorofluorescin-diacetate; JC-1, 5,5′,6,6′-tetrachloro-1,1′,3,3′-tetraethylbenzimidazolcarbocyanine iodide

* Corresponding author. Tel.: +82 62 230 6053; fax: +82 62 233 6052.
E-mail address: seonh@chosun.ac.kr (S.-H. Oh).

0006-2952/$ – see front matter © 2004 Elsevier Inc. All rights reserved.
doi:10.1016/j.bcp.2004.06.021

TNF/Fas-receptor by its ligand leads to the cleavage of procaspase-8, which in turn either directly activates caspase-3 or it induces the cleavage of the BH-3-only Bcl-2 family member p22/Bid to generate p15/tBid, which then subsequently induces cytochrome *c* (Cyt *c*) release [6,7]. Alternatively, there can be diverse proapoptotic signal converge at the mitochondrial level, which will cause the release of Cyt *c* from mitochondria, and Cyt *c* together with Apaf-1 activates caspase-9 and subsequently caspase-3 [8,9]. In these two pathways, a cascade activation of caspases and a release of Cyt *c* from the mitochondria play key roles in these events.

Pro-(Bax, Bid, Bad) and anti-apoptotic Bcl-2 members (Bcl-2, Bcl-X_L) regulate the mitochondrial pathway. Since the anti-apoptotic Bcl-2/Bcl-X_L proteins are localized to the outer mitochondrial membrane, they work to prevent Cyt *c* release from mitochondria [10,11]. Recently, it has reported that the p18/Bax fragment cleaved from full-length Bax (21-kDa) is as efficient as full-length Bax in promoting Cyt *c* release [12–15].

Several investigations have reported that Cd-induced apoptosis occurred via the activation of caspases. In Rat-1 fibroblast cell, Cd induced apoptosis dose- and time-dependently through caspase-3 activation [16]. Zn is a potent caspase-3 inhibitor, and it inhibited Cd-induced apoptosis in C6 rat glioma cells [17,18]. In U-937 promonocytic cells, Cd-induced apoptosis is inhibited by caspase-3 inhibitor. Additionally, in HL-60 cells and human histiocytic lymphoma U937 cells, apoptosis was demonstrated to be mediated by caspase-9 and -8, respectively [19,20]. Furthermore, Shih et al., 2003 [21] demonstrated that in the normal human lung fibroblast cells line, MRC-5, Cd induced apoptosis through mitochondria-mediated AIF translocation into the nucleus, but not via caspase-3 activation and PARP cleavage. In contrast to the above reports, Cd did not induce apoptosis in Chinese hamster ovary (CHO) cells. Cd even blocked apoptosis induced by a metallic challenge (chromium), as well as nonmetallic apoptotic agents such as hygromycin B and actinimycin D, and these two agents are related by their ability to inhibit caspase-3 by Cd [22,23]. Considering the above results surely indicates that the intracellular signaling pathway responsible for Cd-induced apoptosis needs further characterization.

Reactive oxygen species (ROS) have been involved in the apoptosis induced by different stimuli [24,25] as well as the pathologic cell death that occurs in many diseases [26–28]. Some evidence for the participation of ROS in Cd-induced apoptosis were obtained by using antioxidants such as glutathion and catalase [29–31]. On the other hand, Lag et al., 2002 [32] reported that apoptosis induced by cadmium acetate in alveolar type 2 cells and Clara cells isolated from rat lung is not mediated by the oxidative pathway. In CHO cells, Cd even protected against apoptotic cell death that was triggered by a pro-oxidant [22]. Therefore, it remains unclear as to the role of ROS for Cd-induced cytotoxicity.

In this study, to further understand the toxic mechanism of Cd, we investigated the involvement of mitochondria, caspase activation and ROS during Cd-induced apoptosis in WI 38 cells. Our present results show that Cd-induced apoptosis was associated with caspase-dependent Bid cleavage, calpain-mediated mitochondrial Bax cleavage and Cyt *c* release and the reduction of $\Delta\Psi_m$ by ROS production, but apoptosis was independent of Bcl-2.

2. Materials and methods

2.1. Cell culture and drug treatment

The human lung epithelial fibroblast cell line WI 38 cells were maintained in RPMI 1640 medium (GIBCO BRL) and supplemented with heat inactivated 10% fetal bovine serum (GIBCO BRL) and 2 mM L-glutamine (Sigma Chemical Co.) at 37 °C in a 5% CO_2–95% air humidified incubator. The cells were seeded at a density of 1.5×10^6 cells on 10 cm petri dishes and used for the drug exposures after overnight culture, at which time they were approximately 80% confluent. Cadmium acetate [$Cd(Ac)_2$] was purchased from Aldrich Chemical Co. A stock solution of Cd was prepared in PBS and further diluted with RPMI 1640 medium to the desired concentrations. Broad spectrum caspase inhibitor, zVAD-fmk and caspase-8 inhibitor, zIETD-fmk were obtained from Biomol and Calbiochem, respectively.

2.2. MTT cell viability

To determine the cytotoxicity induced by Cd, cells were suspended in RPMI 1640 at 1×10^5 cells/ml. A sample of 100 μl of the cell suspension was seeded into a 96-well plate. After an overnight culture it was replaced with fresh medium containing 0∼80 μM Cd and the cells were further cultured for 24 h. The viability of cultured cells was determined by MTT [3-(4,5-dimethylthiazole-2-yl)-2,5-diphenyltetrazolium bromide, Sigma Chemical Co.] assay [33] and by a tryphan blue exclusion assay.

2.3. Morphological analysis and TUNEL assay

The cells were treated with Cd for 16 h, then washed gently three times with PBS and fixed in neutral buffered formalin for 30 min. The cells were washed with PBS and stained with propidium iodide (PI) solution (50 μg/ml of propidium iodide; 100 μg/ml of RNase A). The morphology of the cells was examined by a Olympus Fluoview laser scanning confocal microscope. Apoptosis was detected by the terminal deoxynucleotidyl transferase-mediated dUTP nick-end labeling (TUNEL) method using the Boehringer in situ death detection kit.

2.4. DNA fragmentation analysis

Fragmented DNA was extracted using a Wizard Genomic DNA purification kit (Promega) according to the described protocol with a slight modification. Briefly, at specific time points after drug treatment, both the floating and adherent cells were pooled in a 1.5 ml tube and lysed for 1 h at 37 °C in a lysis buffer [10 mM Tris–HCl, pH 7.4, 10 mM ethylenediamine tetraacetic acid (EDTA), 0.5% SDS] with 0.5 mg/ml RNase A (Boehringer Mannheim). The DNA was precipitated with ethanol overnight and then it was resuspended in a Tris–EDTA buffer (10 mM Tris, pH 7.4, 1 mM EDTA). Ten μg of the DNA sample was seperated on a 1.2% agarose gel containing 10 μg/ml ethidium bromide and then the DNA band pattern was visualized.

2.5. Determination of ROS production

The production of peroxides was measured by staining cells with DCFH-DA (Molecular probes). This dye is a stable nonpolar compound that readily diffuses into cells and yields DCFH. Intracellular H_2O_2 or OH in the presence of peroxidase change DCFH to the highly fluorescent compound DCF. Thus, the fluorescence intensity is proportional to the amount of peroxides produced by the cells. Following exposure to Cd, cells were incubated in a culture medium containing 20 μM DCFH-DA for 30 min at 37 °C. The fluorescence emission from DCF was detected at 529 nm with the excitation at 503 nm (slit width: 5 nm).

2.6. Measurement of the mitochondrial transmembrane potential ($\Delta\Psi_m$)

The changes in $\Delta\Psi_m$ were monitored with the dye 5,5′,6,6′-tetrachloro-1,1′,3,3′-tetraethylbenzimidazolcarbocyanine iodide (JC-1, Molecular probes). JC-1 emits light at red and green wavelengths according to its concentrations taken up into the mitochondria: at high concentration J-aggregated form emits a red light, whereas at low concentrations the monomer form emits a green light. So the red and green fluoresences of the JC-1 reflect the change of $\Delta\Psi_m$ of the mitochondrial membrane. After the drug treatment, the cells were incubated with JC-1 (3 μM) at 37 °C for 15 min. After washing with PBS, the cells were suspended in the PBS and then observed with a laser scanning confocal microscope (Olympus) and analyzed with flow cytometry (Becton-Dickinson). The green fluorescence from JC-1 monomer (with a 515 nm barrier filter) and the red fluorescence from its J-aggregates (with a 590 nm barrier filter) were visualized simultaneously.

2.7. Preparation of mitochondrial and cytosolic fractions

The cells were washed with ice-cold PBS, then resuspended in ice-cold HMKEE buffer (20 mM HEPES-KOH, pH 7.0, 10 mM KCl, 1.5 mM $MgCl_2$, 1 mM sodium EDTA, 1 mM sodium EGTA, 1 mM dithiothreitol, 0.1 mM phenylmethylsulfonyl fluoride, 10 μg/ml pepstatin A, and 10 μg/ml leupeptin) containing 250 mM sucrose and they were allowed to swell on ice for 20 min. The cells were homogenized by passages through a 26-gauge needle and they were then centrifuged at 14,000 × *g* for 20 min at 4 °C. The cytosolic supernatant was removed and the pellet containing the mitochondria was resuspended in lysis buffer and stored at −70 °C.

2.8. Western blot analysis

At specific time points after the drug treatment, the cells were harvested and washed with PBS and lysed 50 mM HEPES, 150 mM NaCl, 1% Triton X-100, 5 mM EGTA, 50 mM -glycerophosphate, 20 mM NaF, 1 mM Na_3VO_4, 2 mM phenylmethylsulfonyl fluoride, 10 μg/ml leupeptin and 10 μg/ml aprotinin. The cell lysates were centrifuged and the protein content was determined. Equal amounts of protein were separated by SDS-polyacrylamide gel electrophoresis (12–15%), these were transferred to a nitrocellulose membrane and then immunoblotted with the corresponding antibodies. Monoclonal anti-cytochrome *c*, polyclonal anti-caspase-3 and monoclonal anti-poly (ADP-ribose) polymerase (PARP) antibodies were purchased from PharMingen. Polyclonal anti-caspase-8, polyclonal anti-Bid, monoclonal anti-Bcl-2 and polyclonal anti-actin antibodies were obtained from Santa Cruz Biotechnology. Monoclonal anti-calpain 30-kDa subunit and monoclonal anti-p53 antibodies were purchased from Chemicon and NeoMarkers, respectively. The detection of the reacted antigen/antibody products was performed using enhanced chemiluminescence Western Blotting Detection Reagents (Amersham).

2.9. Immunocytochemistry for p53

The cells were cultured on four-chamber polystyrene tissue culture slides (Becton Dickinson) until 90% confluence was achived and then they were exposed to 30 μM Cd for 18 h. After incubation, the cells were washed with PBS, fixed in neutral buffered formalin and washed with PBS several times. Proteins were detected using a Vector laboratory kit. Monoclonal anti-p53 antibody (NeoMakers) was applied to the cells overnight at 4 °C. Alternate chamber was treated with normal serum as a control. After washing them in PBS, the cells were further treated with secondary antibody and their peroxidase activity was detected with AEC (3-amino-9-ethylcarbazole).

2.10. Statistical analysis

Data are expressed as means and standard deviation, and intergroup differences were analyzed using the Student's *t*-test.

3. Results

3.1. Cd-induced apoptosis in WI 38 cells

To examine the Cd's influence on the growth of WI 38 cells, cells were treated with different concentrations of Cd for 24 h. The viability of cells was decreased in a concentration-dependent manner (Fig. 1A). To identify whether Cd was able to induce apoptosis in WI 38 cells, we carried out a morphological analysis using PI and TUNEL staining. As shown in Fig. 1B, in the untreated control cells (a), red fluorescence stained cells with oval-shaped nuclear were seen. The cells that were treated with 40 μM Cd showed a distinct chromatin condensation compare to the control group (b). In a TUNEL analysis, the cells treated with Cd showed a strong intensity of fluorescence (d), indicating a massive DNA breakage, while there was no positive cells in the control group (c). To test further for apoptosis, the DNA fragmentation assay was examined. As shown in Fig. 1C, Cd-induced DNA fragmentation in WI 38 cells in a dose- and time-dependent fashion. In a dose-dependent analysis (a), 10 μM Cd induced a weak fragmentation of DNA. The fragmentation was clearly noted at concentrations of Cd higher than 40 μM, and so we used 40 μM Cd in our present study. In a time-dependent analysis with 40 μM Cd (b), a weak fragmentation was induced at 12 h, but a strong effect was noted at 24 and 36 h.

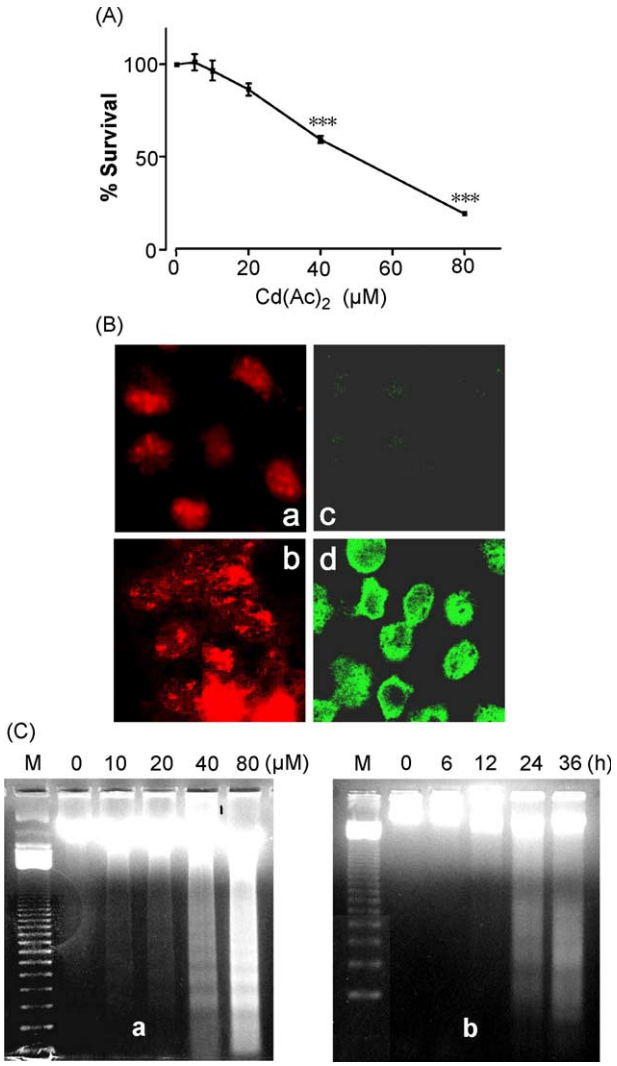

Fig. 1. The effect of cadmium on the viability and apoptotic cell death for WI 38 cells. (A) Dose-dependent inhibition of WI 38 cells growth by cadmium. The cells were incubated with increasing concentration of cadmium for 24 h and cell survival was determined by MTT assay. Values from each point were compared to the control value and they represent the mean ± S.D. of three independent experiments ($^{***}P < 0.005$). (B) The effect of cadmium on chromatin morphology in cadmium-treated WI 38 cells. Panels (a) and (c) show untreated control cells, whereas panels (b) and (d) were treated with 40 μM cadmium for 16 h. The cells were stained PI (a, b) and TUNEL (c, d) as described in Section 2 and observed with confocal microscopy. (C) Concentration- and time-dependent DNA fragmentation of WI 38 cells by cadmium. WI 38 cells were incubated with increasing concentration of cadmium for 24 h (a) and 40 μM of cadmium for the indicated times, respectively. Twenty μg of DNA was run in 1.2% agarose. M: 100 bp DNA ladder.

3.2. Cd-induced ROS production and mitochondrial membrane depolarization

The cytotoxicity of Cd is also related to the production of ROS, and hydrogen peroxide the main ROS involved [21,29]. We measured the level of intracellular ROS in WI 38 cells with Cd. In a time-dependent analysis using 40 μM Cd, the production of ROS was significantly increased at 6 h compared to the control group, with a peak production noted at 24 h (Fig. 2).

ROS production may be accompanied by the reduction of $\Delta\Psi_m$, and so we monitered the change of $\Delta\Psi_m$ in WI 38 cells following a Cd treatment using confocal microscopy and flow cytometry. In the confocal microscopic analysis (Fig. 3A), the untreated control cells showed an intensive red fluorescence (J-aggregate). As the incubation time with Cd increased, the cells increased their green fluorescence (monomer form) and lost their red fluorescence simultaneously. A brighter red functate staining still remained throughout incubation time to 24 h in the living attached cells, but the J-aggregate in the most cells could not be detected at 36 h. This data coincides well with the result of

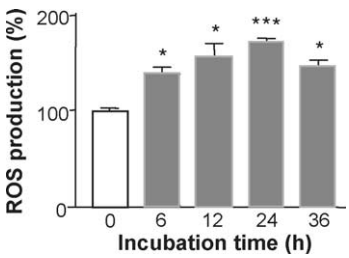

Fig. 2. Cadmium-induced ROS production in WI 38 cells. WI 38 cells were treated with 40 μM of cadmium for the indicated times. ROS intracellular content was analyzed by DCF fluorescence. Values were compared to the vehicle treated control. Results are the means ± S.D. of three independent experiments ($^{*}P < 0.05$; $^{***}P < 0.001$).

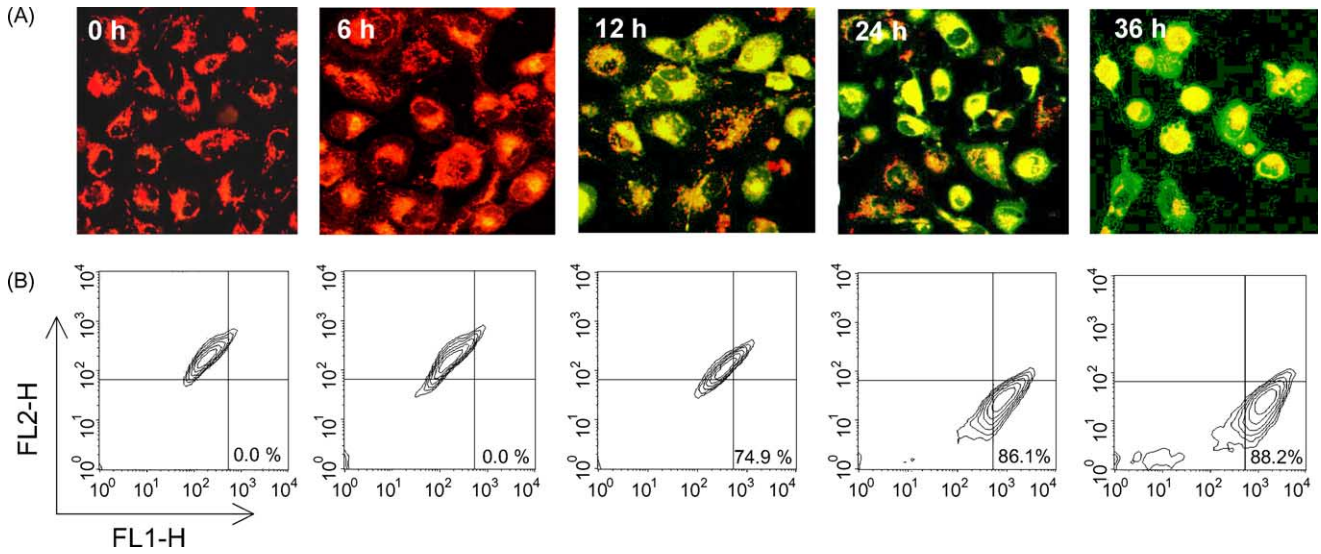

Fig. 3. Mitochondrial transmembrane potential in WI 38 cells treated with 40 μM of cadmium, stained with JC-1 and then analyzed with confocal microscopy and flow cytometry. (A) The untreated control (0 h) shows a strong red fluorcence with a high membrane potential (J-aggregate form of JC-1). But as incubation time with cadmium passed, the cells show a green fluorecence from the monomer form of JC-1. (B) JC-1 fluorecence in the FL-1 channel increased as the mitochondrial membrane potential decreases, while its fluorescence in the FL-2 channel decreases. The percentage numbers (lower-right) indicate the propotion of cells with depolarized mitochondria.

flow cytometry used as a further demonstration. As shown in Fig. 3B, the percentage of cells with the J-monomer (lower-right) increased from 0% of the control cells to 74.9% of Cd-treated cells within 12 h. A drastic change from J-aggreate to J-monomer occurred at 12 h after Cd treatment. To demonstrate the relationship between the production of ROS and reduction of $\Delta\Psi_m$, cells were preincubated with 20 mM *N*-acetylcystein (NAC) for 2 h before treatment with 40 μM Cd. After 10 h of treatment of Cd, the changes of $\Delta\Psi_m$ were measured using JC-1. NAC is able to almost completely inhibit the disruption of $\Delta\Psi_m$ induced by Cd. NAC alone did not affect $\Delta\Psi_m$ (Fig. 4). This result indicates that the reduction of $\Delta\Psi_m$ by Cd could be due to ROS production.

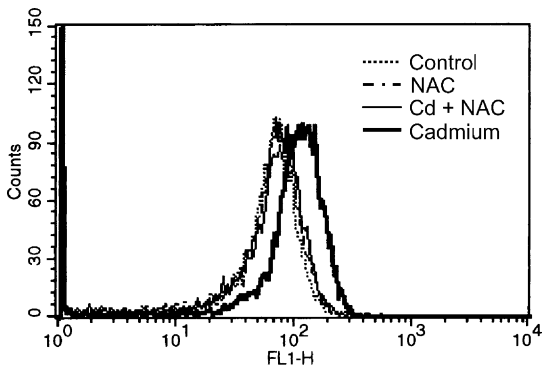

Fig. 4. Effect of *N*-acetylcysteine (NAC) on Cd-induced mitochondrial transmembrane potential ($\Delta\Psi_m$) reduction. Cells were incubated with NAC for 2 h before treatment with 40 μM cadmium. The loss of $\Delta\Psi_m$ was analyzed by flow cytometry after loading with JC-1. The data are representative of three independent experiments giving similar results.

3.3. Cd-induced Cyt *c* release and caspase-9, -3 activation and PARP cleavage

Cyt *c* release is known to be a key event during the mitochondrial-dependent apoptosis, which in turn induces a mitochondrial downstream caspase-9 and -3 activation. Thus, we examined the release of Cyt *c* from the mitochondria into the cytosol. The cells were harvested at the indicated time points following a treatment with 40 μM Cd. Cyt *c* was not detectable in the cytosolic extracts from untreated control cells, whereas the Cd triggered Cyt *c* release to the cytosol (Fig. 5). The amount of Cyt *c* in the cytosol was low at 6 h, but it drastically increased at 12 h. To determine whether the Cyt *c* released from mitochondria was mediated by the activation of caspase-9 and -3, we examined the activation of caspase-9 and -3 by a Western blot analysis. Caspase-9 and -3 began to process after 6 h of Cd treatment, and the activation persisted in a time-dependent manner (Fig. 5). In most of the apoptotic pathway, the activation of caspase-3 causes the cleavage of the PARP to its cleavage form. As shown Fig. 5, PARP began to show cleavage after 12 h.

3.4. Cd activated caspase-8 upstream of the mitochondrial pathway and this induced Bid cleavage

We thought that caspase-8 mediated cleavage of Bid leads to release of Cyt *c* from the mitochondria, and so we carried out a time-dependent analysis of caspase-8 and Bid by Western blot analysis in WI 38 cells treated with Cd (Fig. 5). The activation of procaspase-8 was initiated after 6 h of Cd treatment, and after this time, its intensity

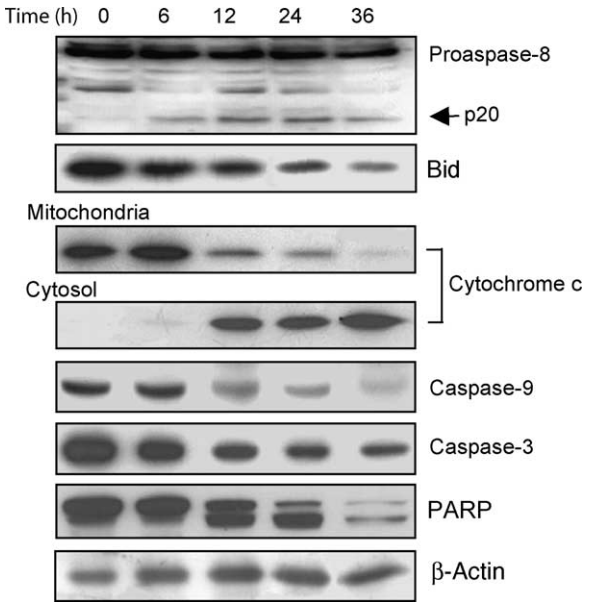

Fig. 5. Cadmium-induced apoptotic signaling pathway in WI 38 cells. The cells were incubated with 40 μM of cadmium for the indicated times. The cells were harvested and lysed. Cytosol and mitochondrial proteins were prepared as described in Section 2. Forty to seventy μg of protein lysate was subjected to 12–15% SDS-PAGE gel and immunoblotted with the corresponding antibodies. Processing of procaspase-8, Bid cleavage, cytochrome *c* release from mitochondria to the cytosol, processing of procaspase-9 and -3, and PARP cleavage were induced by cadmium. β-Actin was used as loading control.

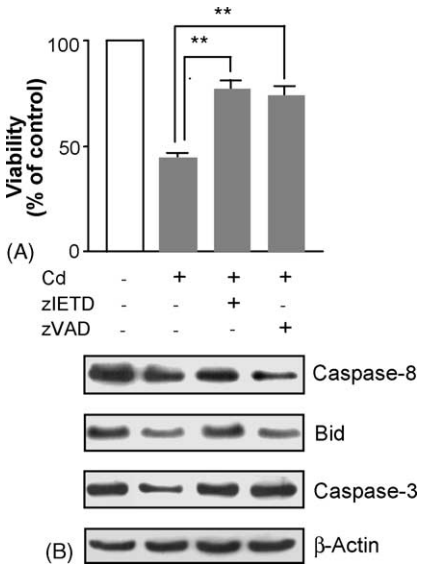

Fig. 6. Cadmium-induced cell death reduced by caspase inhibitors. (A) WI 38 cells were pretreated with 200 μM zIETD-fmk and 40 μM zVAD-fmk for 2 h and then incubated with 30 μM cadmium for 15 h. Cell survival was measured by tryphan blue exclusion. The values are expressed as a percentage compared to the control ($^{**}P < 0.005$). (B) The cells were harvested and lysed. Seventy μg of protein lysate was subjected to 12% SDS-PAGE gel and then immunoblotted with the corresponding antibodies. zIETD-fmk prevented the activation of caspase-8 and -3 by cadmium. β-Actin was used as a loading control.

decreased in a time-dependent manner that corresponded to its cleaved form (p20). The intensity of p21/Bid decreased in a time-dependent manner, and this started at 6 h after Cd treatment. Because caspase-8 functions as an apical initiator of the death-receptor pathway, as well as a target of the caspase-3 downstream pathway of mitochondria, we try to confirm the function of caspase-8. The cells were pretreated with 200 μM of a broad-spectrum caspase inhibitor, zVAD-fmk, and 40 μM of caspase-8 specific inhibitor, zIETD-fmk, for 2 h and the cells were then incubated in 30 μM Cd for 15 h. The pretreatment with both inhibitors significantly attenuated Cd-induced cell death; this was determined by the tryphan blue exclusion (Fig. 6A). In Western blot analysis (Fig. 6B), zIETD-fmk prevented the Bid cleavage and caspase-3 activation, while zVAD-fmk did not prevent the caspase-8 activation and Bid cleavage, indicating that caspase-8 was activated upstream of the mitochondrial pathway.

3.5. Cd induced the cleavage of Bax residing exclusively in the mitochondria

Cd induced the cleavage of the full-length Bax (21- and 24-kDa for BAX_α and BAX_β gene, respectively) into p18/Bax frgments in the whole cell lysates of WI 38 cells (Fig. 7A). The cleavage of full-length Bax was initiated after 12 h, and by 36 h of incubation with Cd the full-length Bax proteins were totally cleaved to the p18/Bax. As previously reported, if the p18/Bax acts as a potent proapoptotic molecule with a Cyt *c* releasing activity, it should be found in a mitochondrial fraction. To test this idea, both cytosolic and mitochondrial factions of WI 38 cells with or without Cd treatment were subjected to a Western blot analysis at the indicated time points. The p18/Bax was detected exclusively in the mitochondrial fraction, but not in the cytosol fraction. The level of p18/Bax in the mitochondrial fraction was upregulated at 12 h, and this matches well with the time of appearance of p18/Bax in the whole cell lysates. In contrast to the mitochondrial fraction, the levels of full-length Bax in the cytosolic fraction were increased at 12 h (Fig. 7A). Therefore, the result suggests that full-length Bax resided only in the mitochondrial fraction and it is cleaved into the p18/Bax, but it is not translocated from cytosolic Bax into the mitochondria.

3.6. Cd-induced mitochondrial calpain activation

Bax has been shown to be cleaved by a Ca^{2+}-activated cystein protease calpain from its full-length p21/Bax form to a p18/bax fragment during apoptosis [12]. Autolysis of the 30-kDa calpain small subunit is associated with calpain activation during apoptosis [34,35]. We examined the expression of 30-kDa calpain small subunit in the cytosolic as well as mitochondrial fraction (Fig. 7B). In whole cell lysates, even though it was detected the autolysis of the calpain small subunit after 6 h of Cd treatment, the level of

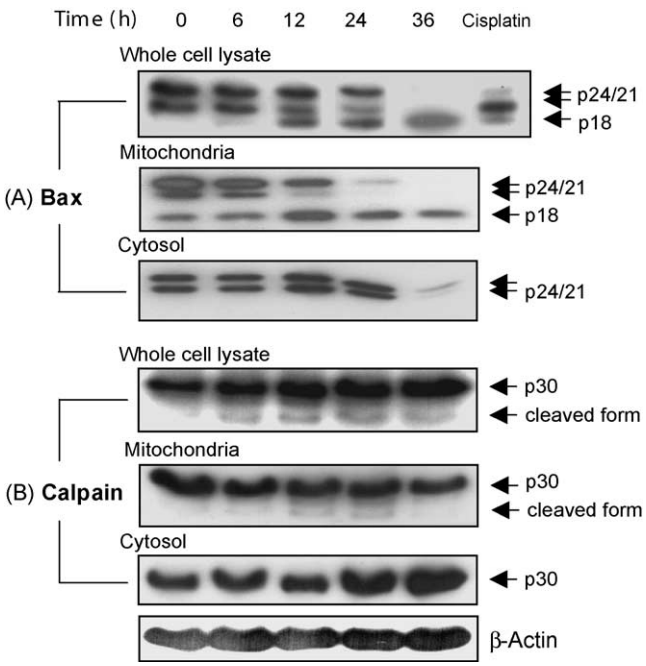

Fig. 7. Cadmium induced mitochondrial Bax cleavage and activation of the mitochondrial calpain small subunit. (A) Anti-Bax antibody (B-9) detected both the full-length Bax (p21, p24/Bax) and the cleaved form of Bax (p18/bax). Upregulation of p18/Bax was detected only in the mitochondrial fraction, not in the cytosol. (B) Activation of the calpain 30-kDa subunit. The intensity of 30-kDa calpain increased with the appearance of the cleaved form at 6 h. In contrast to the cytosolic 30-kDa calpain that showed an increase in a time-dependent fashion, mitochondrial 30-kDa calpain decreased. The cells were incubated with 40 μM cadmium for the indicated times. The cells were harvested, lysed and subjected to 12% SDS-PAGE gel. The proteins were immunoblotted with anti-Bax and anti-calpain for the small subunit antibody, respectively. Cisplatin-treated HepG2 cell lysate and β-actin were used as size marker and loading control, respectively.

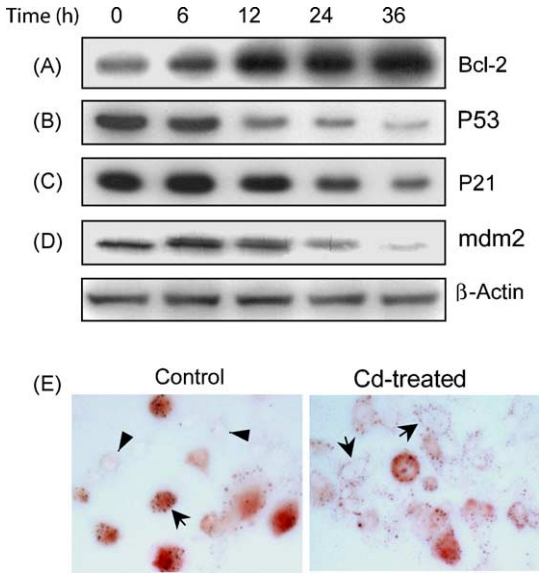

Fig. 8. The change of the expression pattern of apoptosis-related proteins by cadmium. The cells were incubated with 40 μM cadmium for the indicated times. The cells were lysed and immuoblotted with the corresponding antibodies. Cadmium induced the upregulation of Bcl-2 (A) and the down-regulation of p53 (B) and p21 (C). The intensity of mdm2 showed an increase at 6 h, after that, the intensity decreased (D). β-Actin was used as the loading control. (E) Expression pattern and localization of p53 by cadmium in WI 38 cells. After a 40 μM cadmium treatment, the cells were incubated with anti-p53 antibody (Pab 240). Peroxidase activity was detected with AEC. β-Actin was used as a loading control.

calpain small subunit increased in a time-dependent manner. Therefore, we needed to examine this contradiction in the subcellular localization of calpain small subunit. In the mitochondrial fraction, the autolysis of calpain small subunit began at 6 h after Cd treatment with a decrease in the level of 30-kDa subunit, and it persisted for 36 h, while the level of 30-kDa calpain subunit showed an increase in the cytosol.

3.7. Cd-induced apoptosis is independent of the antiapoptotic protein Bcl-2

Since Bcl-2 is mainly located in the outer mitochondrial membrane where it inhibit the membrane's permeability. Furthermore, it has been reported that the expression of anti-apoptotic Bcl-2 suppressed Cd-induced cell death [16,36,37]. To examine the same effect during Cd-induced cell death in WI 38 cells, we carried out a Western blot analysis for Bcl-2 expression. As shown Fig. 8A, in the whole cell lysates, Bcl-2 protein was upregulated in a time dependent manner with Cd treatment. This indicates that Bcl-2 failed to inhibit Cd-induced apoptotic cell death in WI 38 cells.

3.8. Cd-induced rapid degradation of p53

While the p53 is maintained at a low levels through targeted degradation, following damage to the DNA it accumulates in the nucleus and is activated as transcription factors such as *Bax* and *p21 gene* $^{Waf\text{-}1}$ [38–40]. As shown Fig. 8B, p53 protein was expressed at a high basal level and it decreased in a time-dependent manner after Cd treatment. The expression of p53 was further examined by immunocytochemistry (Fig. 8E). In the control cells, many cells showed strong and diffuse intranuclear staining with conspicuous punctate structures, and this indicates the presence of large protein aggregates (arrow), but some cells did not express p53 at all (arrow heads). After a treatment with 30 μM Cd for 18 h, nuclear p53 staining in most of the cells disappeared, but weak punctate structures were randomly dispersed throughout the cytoplasm and at the perinuclear boundary (Fig. 8E, arrows). The functional loss of p53 protein was further supported by p21 protein, a downstream target of p53, by Western blot analysis. The level of p21 protein was also decreased in a time-dependent manner following the Cd treatment (Fig. 8C). In addition, we could detect the induction of mdm2 protein, which is known to partly control p53 inactivation, at 6 h after Cd treatment and then the levels of mdm2 protein showed a decrease (Fig. 8D). These results indicate that Cd-induced degradation of p53 protein through the mdm2 protein

induction in WI 38 cells, thereby inhibiting transcription function of p53 for its downstream targets.

4. Discussion

Epidemiological evidences has shown that occupational and environmental cadmium exposure causes pulmonary damage such as emphysema and lung cancer [41–43]. Although Cd has been demonstrated to induce toxicity via in part by apoptotic cell death, the precise pathway remains poorly understood. In the present study we have attempted to elucidate the molecular events that occurred during Cd-induced cell death in WI 38 cells. Cd activated caspase-8, induced Bid cleavage, caused Cyt *c* release and subsequently, it induced caspase -9 and -3 activation and PARP cleavage. Cd also induced mitochondrial Bax cleavage at a later stage than the time of Bid cleavage. The cleavage of Bax was followed by the autolysis of mitochondrial calpain 30-kDa small subunit. This result suggests that the Cd-induced mitochondrial Bax cleavage is mediated by the activation of calpain. Furthermore, Cd caused ROS production and a reduction of $\Delta\Psi_m$ at early stages after Cd treatment.

Caspases are cystein proteases and they play a key role for cascade activation during apoptosis that is induced by many stimuli. Activation of initiator caspases (procaspase-8, -9, -10) leads to the proteolytic activation of downstream effector caspases (caspase-3, -6, -7). Caspase-8 is an apical caspase that becomes activated upon ligation of the Fas-receptor by its ligand [6,7]. However, Scaffidi et al., 1998 [44] has demonstrated that two different cell types exsits with respect to the Fas apoptosis signaling pathway. Type I cells require activation of caspase-8 early at the DISC (death-inducing signaling complex) and directly followed by activation of caspase-3, and the anti-apoptotic proteins Bcl-2 and Bcl-X_L had no effect on the cleavage of these caspases. On the other hand, in type II cells, caspase-8 was activated downstream of mitochondria, and it was blocked by the overexpression of Bcl-2. Indeed, recent studies on the cytotoxic drug-induced apoptosis pathway have demonstrated that caspase-8 activation is independent of Fas/CD95 signaling and this occurs downstream of caspase-3 [45–47]. Therefore, the results of above authors have led us to study the relationship of a cascade activation of caspases during Cd-induced apoptosis. In our model that used a caspase inhibitor system, we analyzed the activation of caspase-8 and -3 after pretreatment with caspase-8 specific inhibitor zIETD-fmk and broad spectrum caspase-3 inhibitor zVAD-fmk to confirm the function of caspase-8, that is, whether the activation of caspase-8 occurred upstream or downstream of mitochondria. Our results showed that the caspase-8 inhibitor blocked caspase-3 cleavage, while the caspase-3 inhibitor did not prevent the activation of caspase-8. The activation of caspase-8 was inhibited by zIETD-fmk only, but it was not inhibited by zVAD-fmk, which is known to inhibit caspase-1, -3, -4 and -7. This finding indicates that caspase-8 is working as a apical initiator upstream of mitochondria. How Cd activates caspase-8 is not clear. Because ROS can induce Fas and Fas-L expression, and subsequently caspase-8 activation [48], it suggests that Cd-induced ROS may modulate the signal from death-receptor to caspase-8.

Bid, a proapoptotic Bcl-2 family member containing only the BH-3 domain, it is exclusively a cytosolic protein, and it can be cleaved by caspase-8. The cleaved form, tBid, translocates to the mitochondria, where in turn it promote Cyt *c* release [49]. We observed the intensity of a full-length Bid decrease over time following the Cd treatment, and it seems to happen thought the cleavage of Bid to tBid. The Bid cleavage occurred at the same time as the activation of caspase-8 by the Cd treatment, and then tBid triggered a weak release of Cyt *c* from the mitochondria (Fig. 5). This suggests that the caspase-8-dependent Bid cleavage in Cd-induced apoptosis may trigger the mitochondrial pathway by releasing Cyt *c* to induce caspase-9 activation.

It is generally thought that the expression of full-length Bax increased following a death stimulation, and it then translocated into the mitochondria to induce Cyt *c* release [50,51]. Full-length Bax also has been known to undergo post-translational modification during apoptosis in response to various stimuli including Interferon (INF)-α and chemotherapeutic drugs, and the cleaved form of Bax is a potent inducer of apoptotic cell death [52–54]. But the location for the Bax cleavage is not still clear. Lag et al., 2002 [32] reported the upregulationof p53 and Bax expression during Cd-induced apoptosis in alveolar type 2 cells and clara cell from rat lung. To examine above all possibilities including the protein level, post-translational modification and the subcellular localization of Bax by Cd, we examined the level of Bax in whole cell lysates in mitochondrial and cytosol fractions during Cd-induced apoptosis. Our results showed that the level of full-length Bax protein in the whole cell lysates decreased in a time-dependent manner with upregulation of the p18/Bax fragment at 12 h after Cd treatment (Fig. 7A). This suggests that p18/Bax may be involved in the apoptotic signaling pathway by Cd in WI 38 cells. For Bax is localized in both cytosol and mitochondrial membrane [49,55], the mitochondrial p18/Bax could be originating from the cleavage of either the mitochondrial full-length or cytosolic full-length Bax. However, only the mitochondrial full-length Bax decreased corresponding to the upregulation the p18/Bax at 12 h, and this indicates that mitochondrial Bax may be cleaved by some factors located in mitochondria or translocated from cytosol after Cd treatment. In contrast to the mitochondrial fraction, cytosolic full-length Bax showed an increase at 12 h after Cd treatment, indicating that cytosolic Bax did not translocate into the mitochondria.

As we noted, the p18/Bax fragment is a potent inducer of Cyt *c* release. In our present study, Cyt *c* was drastically released from mitochondria after 12 h of Cd treatment (Fig. 5), which was coincidental with the timing of Bax cleavage in the mitochondrial fraction after Cd treatment (Fig. 7A). This indicates that the cleavage of Bax plays a critical role in releasing Cyt *c* during Cd-induced apoptosis. Therefore, our results suggest that there is a possibility that at the later stage, the p18/Bax can synergically works with Bid cleaved at the early stage to induce Cyt *c* release from mitochondria after Cd treatment. If so, we thought about what could be the factor related with Bax cleavage after the Cd treatment. Since Wood et al., 1998 [54] has demonstrated that calpain is involved in the cleavage of full-length Bax during drug-induced apoptosis, several investigations have reported that the cleavage of Bax by calpain generates a potent proapoptotic p18/Bax [13–15,56]. Gao and Dou, 2000 [13] demonstrated that activation of the calpain is a prerequisite for Bax cleavage. They also found that the activation of the calpain small subunit in the mitochondrial is required for apoptosis execution [35]. In our present study, even though the intensity of 30-kDa calpain subunit in the whole cell lysates showed an increase in a time-dependent manner, this was accompanied by autolysis/activation of calpain after 6 h by the Cd treatment. The answer for this contradiction could be found by examing the subcellular localization of 30-kDa calpain. The 30-kDa calpain in the mitochondrial fraction showed a decrease with the appearance of the cleaved form after 6 h of incubation with Cd. In contrast to the mitochondrial fraction, the 30-kDa calpain increased in the cytosol. This result indicates that mitochondrial Bax cleavage is mediated by activation of the mitochondrial calpain (Fig. 7B).

ROS includes the superoxide (O_2^-), hydroxyl radicals and hydrogen peroxide (H_2O_2), and ROS may act as a signal molecule of the death pathway [24,25]. Several investigations have been demonstrated that the cytotoxicity by Cd is associated with ROS [21,57,58], and ROS production results in mitochondrial membrane depolarization. In a time-course analysis for ROS, the production of ROS significantly increased after 6 h of Cd treatment, after this it continuously increased for 24 h (Fig. 2). The change of $\Delta\Psi_m$ at the same time points showed a drastic change of fluorescence after 12 h of Cd treatment. Furthermore, the experiment using NAC, a precursor of glutathione, demonstrated that ROS production is preceded by the reduction of $\Delta\Psi_m$ (Fig. 4). Though we did not confirm the role of ROS in cell viability, the increased ROS production by Cd may led to the reduction of $\Delta\Psi_m$. This in turn increases mitochondrial membrane permeability (MMP) and subsequently, there is a release of mitochondrial apoptogenic factors into cytosol.

Anti-apoptotic Bcl-2 family member proteins such as Bcl-2 and Bcl-X_L inhibit the proapoptotic function of Bax, as well as apoptotic cell death associated with oxidants [59–61]. Furthermore, it has been demonstrated that Cd-induced cell death is suppressed by Bcl-2 [16,36,37]. In our present study, although Cd induced an increase of Bcl-2 protein in a time-dependent manner in whole cell lysates (Fig. 8A), it did not prevent Cd-induced apoptotic cell death in WI 38 cells. Therefore, our results suggest that Bcl-2 did not interact with the mitochondrial p18/Bax in WI 38 cells. Indeed, Gao and Dou, 2000 [13] demonstrated that the potent proapoptotic p18/Bax was independent of Bcl-2.

The tumor suppressor p53 is activated upon DNA damage and it is accumulated in the nucleus, where it then functions as transcription regulator for its downstream target genes such as *p21* and *Bax* [38–40]. In normal cells, p53 levels are tightly regulated because of a short half-life [62] and they are not detectable by immunocytochemistry. Leg et al., 2002 [32] reported an increase of p53 and Bax expression by Cd in the lung type II alveolar and clara cells of rat. On the other hand, Méplan et al., 1999 [63] reported that in human breast cancer MCF7 cells, Cd induced a conformational change of the p53 structure, and thereby inhibited its DNA binding ability and inactivated the p53 protein. These authors also suggested, that in contrast to the accumulation of p53 protein at low concentration (up to 10 μM), 40 μM of Cd caused a significant decrease of p53 protein. In our present study, we observed a decrease of p53 protein in a time-dependent manner following 40 μM Cd treatment, and also, we could not observe the upregulation of the downstream effector proteins such as p21 and Bax (Figs. 6 and 7). The functional inactivation of p53 strongly correlates with tumorigenesis and it is the result of at least two mechanisms; mutational inactivation is the most common mechanism and it is found in many types of cancers leading to nuclear accumulation [64]. The other is mutational-independent mechanisms that include cytoplasmic sequestration by viral oncoproteins [65,66] and degradation by HPV-16/18 E6 oncoprotein and mdm2 [67,68]. Once protein stabilization is occurrs by mutation or by post-transcriptional modification of the wild-type p53, this results in the upregulation of p53 protein by nuclear accumulation or cytoplasmic sequestration and it becomes detectable by immunocytochemistry. However, we could not observe the same effect by Western blot analysis and immunocytochemistry (Fig. 8B and E). Therefore, we could exclude the possibility that the loss of p53 function was caused by mutation or post-transcriptional modification of p53 after Cd treatment. In view of our present data, a more attractive explanation for the decrease of p53 protein by Cd is that it is thought to be caused by degradation. This idea was supported by the upregulation of mdm2 protein at 6 h after Cd treatment (Fig. 8D). Therefore, our results suggest that Cd can effectively inhibit p53 function through the degradation of p53 protein.

When taken together, our results suggest that Cd might induce Cyt *c* release via at least two different apoptotic pathways. One pathway is that the caspase-dependent Bid

cleavage caused a weak Cyt *c* release from mitochondria at the early stage. The other pathway is that there is a calpain-mediated mitochondrial Bax cleavage at a later stage of Cd treatment, which synergistically works with Bid, and so it caused a drastic Cyt *c* release from mitochondria. The proapoptotic function of Bid and Bax was not prevented by Bcl-2. Cd can suppress the p53 activation by inducing degradation of p53 protein. NAC inhibited Cd-induced $\Delta\Psi_m$ reduction, indicating ROS acts upstream of mitochondrial membrane depolarization.

Acknowledgments

This study was supported by grants from Ministry of Science and Technology, Korea, and from Korea Science and Engineering Foundation through the Research Center for Resistant Cells. We would like to thank Ms. Y.K. Soo and T.B. Lee for technical assistance and Dr. H.J. Jang of the Jang Hyo-Juk Cosmetic Clinic for helpful discussions.

References

[1] IARC, International Agency for Research on Cancer. Monographs on the Evaluation of the Carcinogenic Risks to Humans, vol. 58, Beryllium, Cadmium, Mercury and Exposures in the Glass Manufacturing Industry. Lyon, France: IARC Scientific Publications; 1993. p. 119–238.

[2] Hayes JA. Metal toxicity. In: Marquis JK, editor. A Guide to General Toxicity. Basel: Karger; 1989. p. 179–278.

[3] Nandi M, Slone D, Jick H, Shapiro S, Lewis GP. Cadmium content of cigarettes. Lancet 1969;2:329–30.

[4] Schwartzman RA, Cidlowski JA. Apoptosis: the biochemistry and molecular biology of programmed cell death. Endocr Rev 1993;4: 133–51.

[5] Thompson CB. Apoptosis in the pathogenesis and treatment of disease. Science 1995;267:1456–62.

[6] Kischkel FC, Hellbardt S, Behrmann I, Germer M, Pawlita M, Krammer PH, et al. Cytotoxicity-dependent APO-1(Fas/CD95)-associated proteins form a death-inducing signaling complex (DISC) with the receptor. EMBO J 1995;14:5579–88.

[7] Fulda S, Meyer E, Friesen C, Susin SA, Kroemer G, Debatin KM. Cell type specific involvement of death receptor and mitochondrial pathways in drug-induced apoptosis. Oncogene 2001;20:1063–75.

[8] Sun XM, MacFarlane M, Zhuang J, Wolf BB, Green DR, Cohen GM. Distinct caspase cascades are inhibited in receptor-mediated and chemical-induced apoptosis. J Biol Chem 1999;274:5053–60.

[9] Gross A, McDonnell JM, Korsmeyer SJ. Bcl-2 family members and the mitochondria in apoptosis. Genes Dev 1999;13:1899–911.

[10] Krajewski S, Tanaka S, Takayama S, Schibler MJ, Fenton W, Reed JC. Investigation of the subcellular distribution of the Bcl-2 oncoprotein: residence in the nuclear envelope, endoplasmic reticulum, and outer mitochondrial membranes. Cancer Res 1993;53:4701–14.

[11] Green DR, Reed JC. Mitochondria and apoptosis. Science 1998;281: 1309–12.

[12] Wood DE, Newcomb EW. Caspase-dependent activation of calpain during drug-induced apoptosis. J Biol Chem 1999;274:8309–15.

[13] Gao G, Dou QP. N-terminal cleavage of Bax by calpain generates a potent proapoptotic 18-kDa fragment that promotes Bcl-2-independent cytochrome c release and apoptotic cell death. J Cell Biochem 2000;80:53–72.

[14] Toyota H, Yanase N, Yoshimoto T, Moriyama M, Sudo T, Mizuchi J. Calpain-induced Bax-cleavage product is a more potent inducer of apoptotic cell death than wild-type Bax. Cancer Lett 2003;189:221–30.

[15] Daniel KG, Anderson JS, Zhong Q, Kazi A, Gupta P, Dou QP. Association of mitochondrial calpain activation with increased expression and autolysis of calpain small subunit in an early stage of apoptosis. Int J Mol Med 2003;12:247–52.

[16] Kim MS, Kim BJ, Woo HN, Kim KW, Kim KB, Kim IK, et al. Cadmium induces caspase-mediated cell death: suppression by Bcl-2. Toxicology 2000;145:27–37.

[17] Perry DK, Smyth MJ, Stennicke HR, Salvesen GS, Duriez P, Poirier GG, et al. Zinc is a potent inhibitor of the apoptotic protease, caspase-3. A novel target for zinc in the inhibition of apoptosis. J Biol Chem 1997;272:18530–3.

[18] Watjen W, Haase H, Biagioli M, Beyersmann D. Induction of apoptosis in mammalian cells by cadmium and zinc. Environ Health Perspect 2002;xx(Suppl. 110):865–7.

[19] Li M, Kondo T, Zhao QL, Li FJ, Tanabe K, Arai Y, et al. Apoptosis induced by cadmium in human lymphoma U937 cells through Ca^{2+}-calpain and caspase-mitochondrial-dependent pathways. J Biol Chem 2000;275:39702–9.

[20] Kondoh M, Araragi S, Sato K, Higashimoto M, Takiguchi M, Sato M. Cadmium induces apoptosis partly via caspase-9 activation in HL-60 cells. Toxicology 2002;170:111–7.

[21] Shih CM, Wu JS, Ko WC, Wang LF, Wei YH, Liang HF, et al. Mitochondria-mediated caspase-independent apoptosis induced by cadmium in normal human lung cells. J Cell Biochem 2003;89: 335–47.

[22] Shimada H, Shiao YH, Shibata M, Waalkes MP. Cadmium suppresses apoptosis induced by chromium. J Toxicol Environ Health A 1998;54:159–68.

[23] Yuan C, Kadiiska M, Achanzar WE, Mason RP, Waalkes MP. Possible role of caspase-3 inhibition in cadmium-induced blockage of apoptosis. Toxicol Appl Pharmacol 2000;164:321–9.

[24] Tan S, Sagara Y, Liu Y, Maher P, Schubert D. The regulation of reactive oxygen species production during programmed cell death. J Cell Biol 1998;141:1423–32.

[25] Simon HU, Haj-Yehia A, Levi-Schaffer F. Role of reactive oxygen species (ROS) in apoptosis induction. Apoptosis 2000;5:415–8.

[26] Halliwell B. Reactive oxygen species and the central nervous system. J Neurochem 1992;59:1609–23.

[27] Ames BN, Shigenaga MK, Hagen TM. Oxidants, antioxydants and the degenerative diseases of aging. Proc Natl Acad Sci USA 1993;90: 7915–7922.

[28] Shigenaga MK, Hagen TM, Ames BN. Oxydative damage and mitochondrial decay in aging. Proc Natl Acad Sci USA 1994; 91:10771–8.

[29] Yang CF, Shen HM, Shen Y, Zhuang ZX, Ong CN. Cadmium-induced oxidative cellular damage in human fetal lung fibroblasts (MRC-5 cells). Environ Health Perspect 1997;105:712–6.

[30] Hart BA, Lee CH, Shukla GS, Shukla A, Osier M, Eneman JD, et al. Characterization of cadmium-induced apoptosis in rat lung epithelial cells: evidence for the participation of oxidant stress. Toxicology 1999;133:43–58.

[31] Chuang SM, Wang IC, Hwua YS, Yang JL. Short-term depletion of catalase suppresses cadmium-elicited c-Jun N-terminal kinase activation and apoptosis: role of protein phosphatases. Carcinogenesis 2003;24:7–15.

[32] Lag M, Westly S, Lerstad T, Bjornsrud C, Refsnes M, Schwarze PE. Cadmium-induced apoptosis of primary epithelial lung cells: involvement of Bax and p53, but not of oxidative stress. Cell Biol Toxicol 2002;18:29–42.

[33] Monks A, Scudiero D, Skehan P, Shoemaker R, Paull K, Vistica D, et al. Feasibility of a high-flux anticancer drug using a diverse panel of cultured human tumor cell lines. J Natl Cancer Inst 1991;83: 757–66.

[34] Nath R, Raser KJ, Stafford D, Hajimohammadreza I, Posner A, Allen H, et al. Non-erythroid/alpha-spectrin breakdown by calpain and interleukin 1 beta-converting enzyme-like protease(s) in apoptotic cell: contributory roles of both protease families in neuronal apoptosis. Biochem J 1996;319:683–90.
[35] Daniel KG, Anderson JS, Zhong Q, Kazi A, Gupta P, Dou QP. Association of mitochondrial calpain activation with increased and autolysis of calpain small subunit in an early stage of apoptosis. Int J Mol Med 2003;12:247–52.
[36] Biagioli M, Watjen W, Beyersmann D, Zoncu R, Cappellini C, Ragghianti M, et al. Cadmium-induced apoptosis in murine fibroblasts is suppressed by Bcl-2. Arch Toxicol 2001;75:313–20.
[37] Ishido M, Ohtsubo R, Adachi T, Kunimoto M. Attenuation of both apoptotic and necrotic actions of cadmium by Bcl-2. Environ Health Perspect 2002;110:37–42.
[38] El-Deiry WS, Tokino T, Velculescu VE, Levy DB, Parsons R, Trent JM, et al. WAF1, a potential mediator of p53 tumor suppression. Cell 1993;75:817–25.
[39] Wu X, Bayle JH, Olson D, Levine AJ. The p53-mdm-2 autoregulatory feedback loop. Genes Dev 1993;7:1126–32.
[40] Miyashita T, Reed JC. Tumor suppressor p53 is a direct transcriptional activator of the human bax gene. Cell 1995;80:293–9.
[41] Dervan PA, Hayes JA. Peribronchiolar fibrosis following acute experimental lung damage by cadmium aerosol. J Pathol 1979;128:143–9.
[42] Hirano S, Tsukamoto N, Higo S, Suzuki KT. Toxicity of cadmium oxide instilled into the rat lung II. Inflammatory responses in bronchoalveolar lavage fluid. Toxicology 1989;55:25–35.
[43] Driscoll KE, Maurer JK, Poynter J, Higgins J, Asquith T, Miller NS. Stimulation of rat alveolar macrophage fibronectin release in a cadmium chloride model of lung injury and fibrosis. Toxicol Appl Pharmacol 1992;116:30–7.
[44] Scaffidi C, Fulda S, Srinivasan A, Friesen C, Li F, Tomaselli KJ, et al. Two CD95 (Apo-1/Fas) signaling pathways. EMBO J 1998;17:1675–87.
[45] Chen Q, Gong B, Almasan A. Distinct stages of cytochrom c release from mitochondria: evidence for a feedback amplification loop linking caspase activation to mitochondrial dysfunction in genotoxic stress induced apoptosis. Cell Death Differ 2000;7:227–33.
[46] Wieder T, Essmann F, Prokop A, Schmelz K, Schulze-Osthoff K, Beyaert R, et al. Activation of caspase-8 in drug-induced apoptosis of B-lymphoid cells is independent of CD95/Fas receptor–ligand interaction and occurs downstream of caspase-3. Blood 2001;97:1378–87.
[47] von Haefen C, Wieder T, Essmann F, Schulze-Osthoff K, Dorken B, Daniel PT. Paclitaxel-induced apoptosis in BJAB cells proceeds via a death receptor-independent, caspases-3/-8-driven mitochondrial amplification loop. Oncogene 2003;22:2236–47.
[48] Denning TL, Takaishi H, Crowe SE, Boldogh I, Jevnikar A, Ernst PB. Oxidative stress induces the expression of Fas and Fas ligand and apoptosis in murine intestinal epithelial cells. Free Radic Biol Med 2002;33:1641–50.
[49] Li H, Zhu H, Xu CJ, Yuan J. Cleavage of BID by caspase-8 mediates the mitochondrial damage in the Fas pathway of apoptosis. Cell 1998;94:491–501.
[50] Wolter KG, Hsu YT, Smith CL, Nechushtan A, Xi XG, Youle RJ. Movement of Bax from the cytosol to mitochondria during apoptosis. J Cell Biol 1997;139:1281–92.
[51] Putcha GV, Deshmukh M, Johnson Jr EM. Bax translocation is a critical event in neuronal apoptosis: regulation by neuroprotectants, Bcl-2, and caspases. J Neurosci 1999;19:7476–85.
[52] Thomas A, El Rouby S, Reed JC, Krajewski S, Silber R, Potmesil M, et al. Drug induced apoptosis in B-cell chronic lymphocytic leukemia: relationship between p53 gene mutation and bcl-2/bax proteins in drug resistance. Oncogene 1996;12:1055–62.
[53] Yanase N, Takada E, Yoshihama I, Ikegami H, Mizuguchi J. Participation of Bax-alpha in IFN-alpha-mediated apoptosis in Daudi B lymphoma cells. J Interferon Cytokine Res 1998;18:855–61.
[54] Wood DE, Thomas A, Devi LA, Berman Y, Beavis RC, Reed JC, et al. Bax cleavage is mediated by calpain during drug-induced apoptosis. Oncogene 1998;17:1069–78.
[55] Hsu YT, Wolter KG, Youle RJ. Cytosol-to-membrane redistribution of Bax and Bcl-x_L during apoptosis. Proc Natl Acad Sci USA 1997;94:3668–72.
[56] Cao X, Deng X, May WS. Cleavage of Bax to p18 Bax accelerates stress-induced apoptosis, and a cathepsin-like protease may rapidly degrade p18 Bax. Blood 2003;102:2605–14.
[57] Risso-de Faverney C, Devaux A, Lafaurie M, Girard JP, Bailly B, Rahmani R. Cadmium induces apoptosis and genotoxicity in rainbow trout hepatocytes through generation of reactive oxygen species. Aquat Toxicol 2001;53:65–76.
[58] Watanabe M, Henmi K, Ogawa K, Suzuki T. Cadmium-dependent generation of reactive oxygen species and mitochondrial DNA breaks in photosynthetic and non-photosynthetic strains of *Euglena gracilis*. Comp Biochem Physiol C 2003;134:227–34.
[59] Oltvai ZN, Milliman CL, korsmeyer SJ. Bcl-2 heterodimerizes in vivo with a conserved homologue, Bax, that accelerates programmed cell death. Cell 1993;74:609–19.
[60] Hockenbery DM, Oltvai ZN, Yin XM, Milliman CL, Korsmeyer SJ. Bcl-2 functions in an antioxidant pathway to prevent apoptosis. Cell 1993;75:241–51.
[61] Lee YJ, Chen JC, Amoscato AA, Bennouna J, Spitz DR, Suntharalingam M, et al. Protective role of Bcl-2 in metabolic oxidative stress-induced cell death. J Cell Sci 2001;114:677–84.
[62] Oren M, Maltwman W, Levine AJ. Post-translational regulation of the 54k cellular tumor antigen in normal and transformed cells. Mol Cell Biol 1981;1:101–10.
[63] Méplan C, Mann K, Hainaut P. Cadmium induces conformational modifications of wild-type p53 and suppresses p53 response to DNA damage in cultured cells. J Biol Chem 1999;274:31663–70.
[64] Harris CC, Hollstein M. Clinical implication of the p53 tumor-suppressor gene. N Engl J Med 1993;329:1318–27.
[65] Mietz JA, Unger T, Huibregtse JM, Howley PM. The transcriptional transactivation function of wild-type p53 is inhibited by SV40 large T-antigen and by HPV-16 E6 oncoprotein. EMBO J 1992;11:5013–20.
[66] Debbas M, White E. Wild-type p53 mediates apoptosis by ElA, which is inhibited by ElB. Genes Dev 1993;7:546–54.
[67] Momand J, Zambetti GP, Olson DC, George D, Levine AJ. The mdm-2 oncogene product forms a complex with the p53 protein ad inhibits p53-mediated transactivation. Cell 1992;69:1237–45.
[68] Freedman DA, Levine AJ. Nuclear export is required for degradation of endogenous p53 by MDM2 ad human papillomavirus E6. Mol Cell Biol 1998;18:7288–93.